Supporting Information for "Bias Corrected Estimation of Paleointensity (BiCEP): An improved methodology for obtaining paleointensity estimates"

Brendan Cych[1], Matthias Morzfeld[1], Lisa Tauxe[1]

[1]University of California, San Diego

[1]9500 Gilman Drive, La Jolla, CA, 92093, USA

Contents of this file

1. Figure S1- plots of B_{exp} vs B_{anc} results using the BiCEP method and other sets of selection criteria used in this study.

2. Figure S2- plots of the credible intervals of BiCEP results for subsamples of 5 specimens from sites hw108, VM and hw123.

3. Figures S3 to S32- plots of unpooled B_{anc} and $\vec{k}$ fits and the BiCEP method applied to all sites used in this study.

Additional Supporting Information (Files uploaded separately)

1. Caption for Data Set S1 - This dataset contains the full set of results shown in Figure 7 and described in Section 3.

Data Set S1

This data set is a csv file containing the full set of results for each version of the BiCEP method (Linear, Quadratic and Cubic models with 5, 10 and 20 μT standard deviations

on the prior for σ_{site}, vs classic selection criteria. Columns are named by the model class (Linear, Quadratic, Cubic, or Selection Criteria, followed by the criteria name/prior standard deviation in μT) and then the parameter in question, either the percentile (2.5%, 50%, 97.5%) or f_prob for the f_{prob} value. The first three columns of the csv file contain the site name, B_{exp} and number of specimens (M).

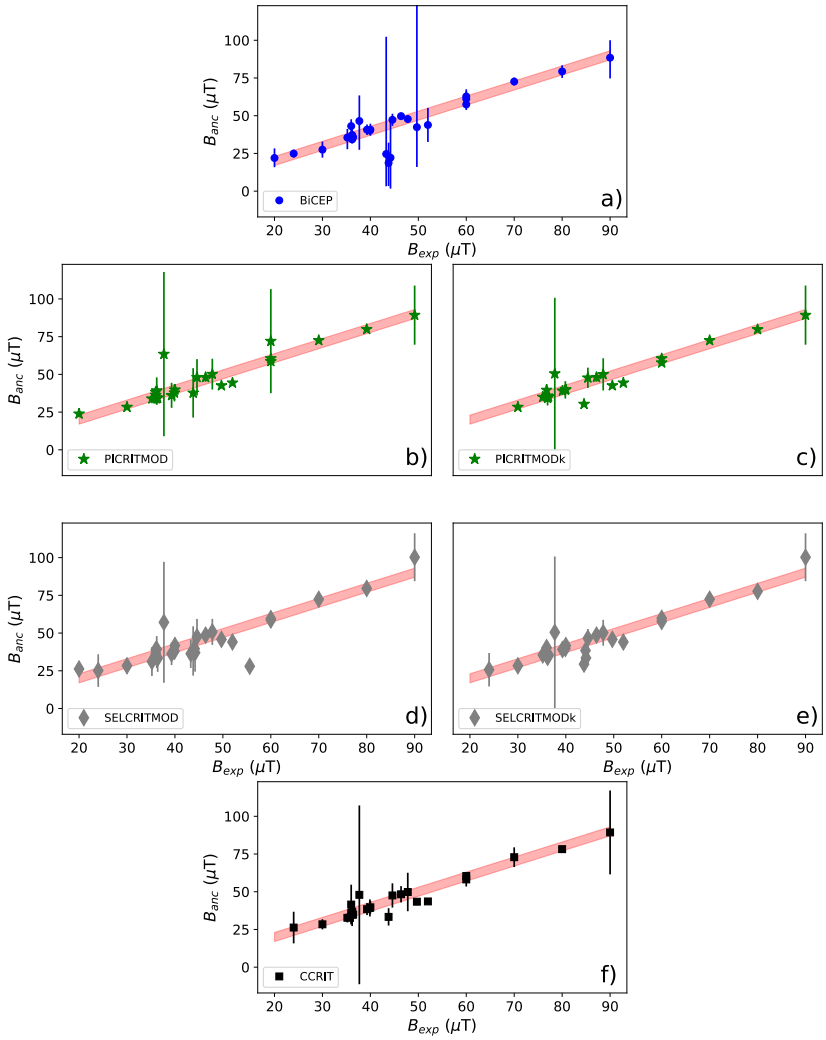

Figure S1. Plot of B_{anc} vs B_{exp} for the passing sites for BiCEP and each of our criteria. a) BiCEP results, b) PICCRITMOD results, c) PICRITMODk results, d) SELCRIT results, e) SELCRITMODk results, f) CCRIT results. Red shaded area represents B_{exp} ± 3 μT. Note that for BiCEP, most of the severely underestimated and highly inaccurate results are for sites with low numbers of specimens ($M < 5$) which did not pass the other criteria.

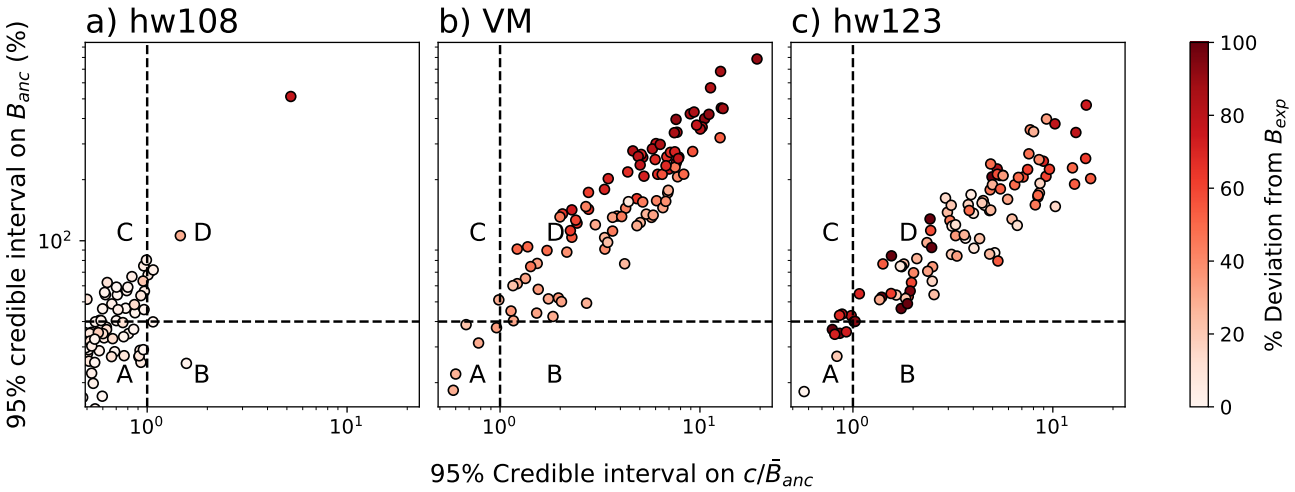

Figure S2. Figure in the style of Figure 9 from the main manuscript. A set of 100 random subsamples of 5 specimens were taken from a) site hw108, b) site VM and c) site hw123. We applied the BiCEP method to these subsamples and plot the 95% credible interval on B_{anc} as a percentage against the 95% credible interval on $c/\tilde{B}_{anc}$. Dashed lines represent the boundaries between regions A, B, C and D, defined in Section 4.3, and point colors represent the percentage deviation of the median from B_{exp}. It is apparent that for our sites where we obtain an inaccurate answer for a large number of specimens (VM and $hw123$), our subsamples fall in region D the majority of the time (94/100 and 90/100 respectively). Conversely, our site hw108, which returns an accurate result with higher numbers of specimens only has 5 results in region D. This indicates that we should either continue measuring specimens (region C, 24/100 results) or that we have a relatively accurate and precise result already (regions A and B, 66/100 results). Although few sites/subsamples were used for this analysis, this test indicates that our labelling scheme has a predictive accuracy of 90-95%

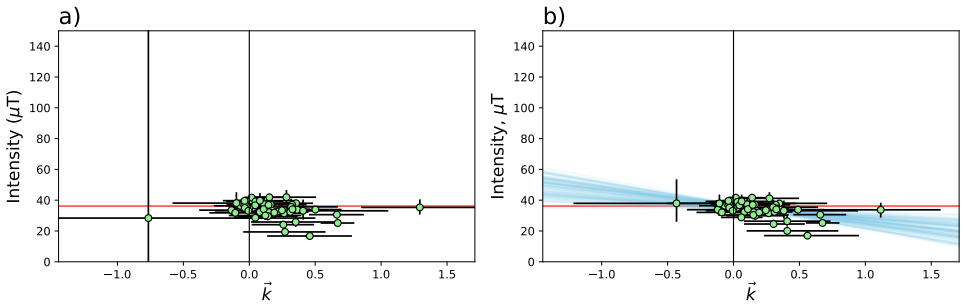

Figure S3. Unpooled and BiCEP models applied to site 1991-1992 Eruption Site a). Independent estimates of B_{anc} vs $\vec{k}$ are plotted as green circles. These estimates are made without assuming a linear relationship between B_{anc} and $\vec{k}$, similar to the analysis in Figure 9a) Black error bars represent 95% credible intervals. b) The BiCEP method applied to this site. Green circles and error bars represent the 95% credible interval, blue lines represent draws from the posterior distribution. The $\vec{k}$=0 axis is plotted as a black vertical line, and the value of B_{exp} is plotted as a red horizontal line. For an accurate estimate, the blue lines should cross the point where these two lines intersect.

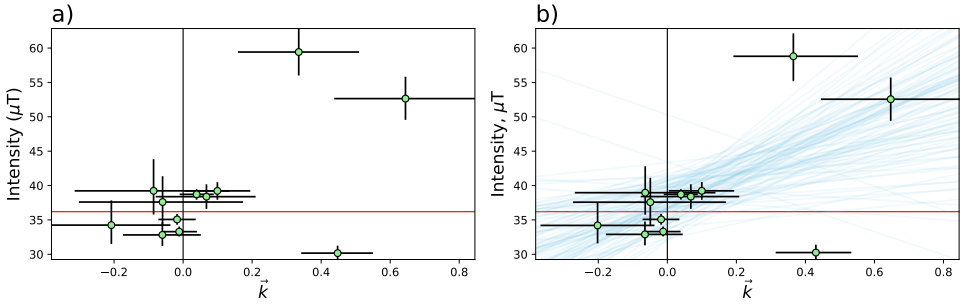

Figure S4. The same methodology described in the caption for Figure S3 applied to site BBQ

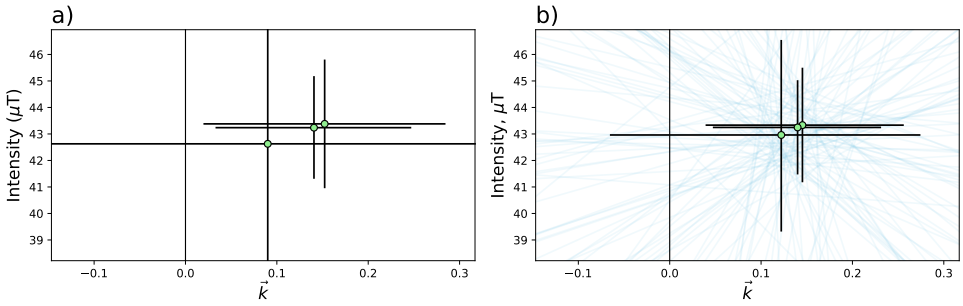

Figure S5. The same methodology described in the caption for Figure S3 applied to site BR06

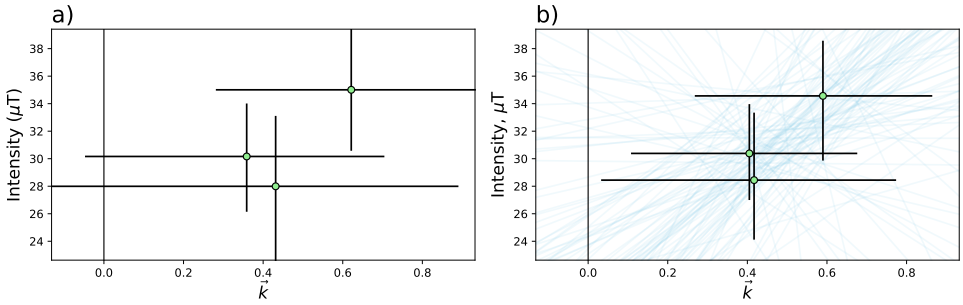

Figure S6. The same methodology described in the caption for Figure S3 applied to site ET1

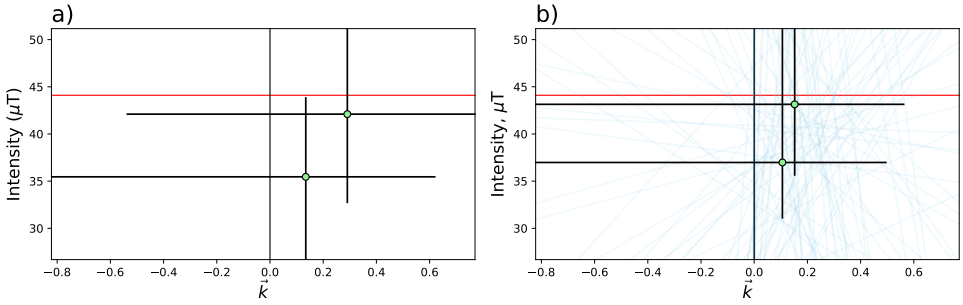

Figure S7. The same methodology described in the caption for Figure S3 applied to site ET2

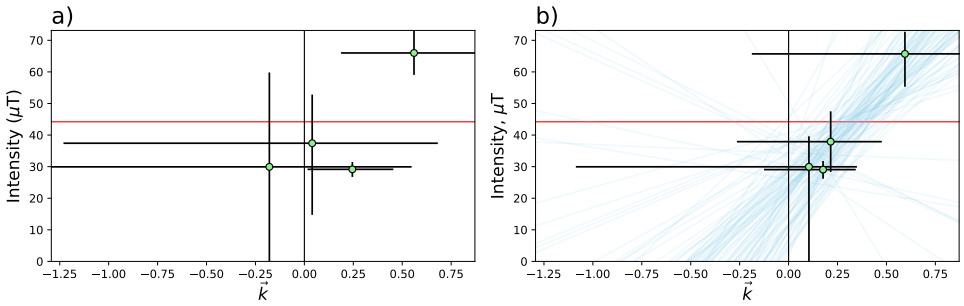

Figure S8. The same methodology described in the caption for Figure S3 applied to site ET3

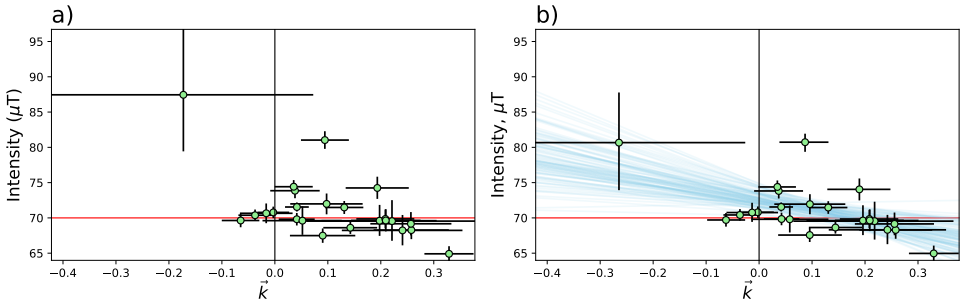

Figure S9. The same methodology described in the caption for Figure S3 applied to site FreshTRM

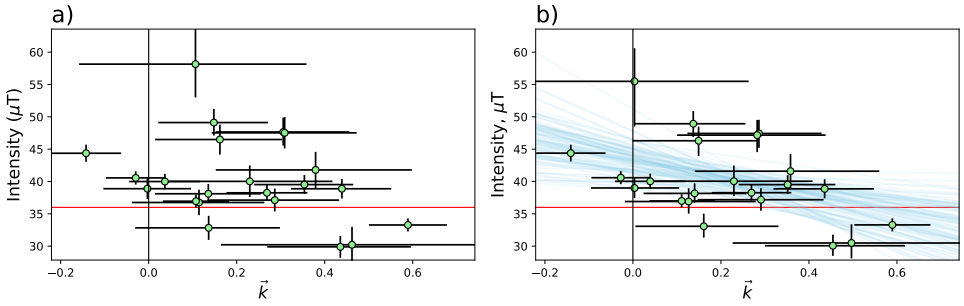

Figure S10. The same methodology described in the caption for Figure S3 applied to site Hawaii 1960 Flow

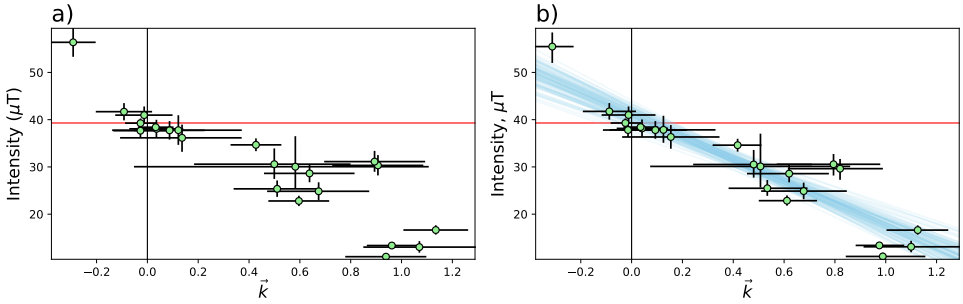

Figure S11. The same methodology described in the caption for Figure S3 applied to site hw108

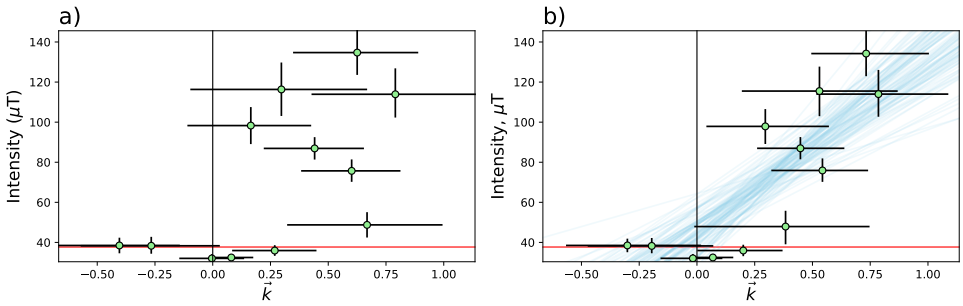

Figure S12. The same methodology described in the caption for Figure S3 applied to site hw123

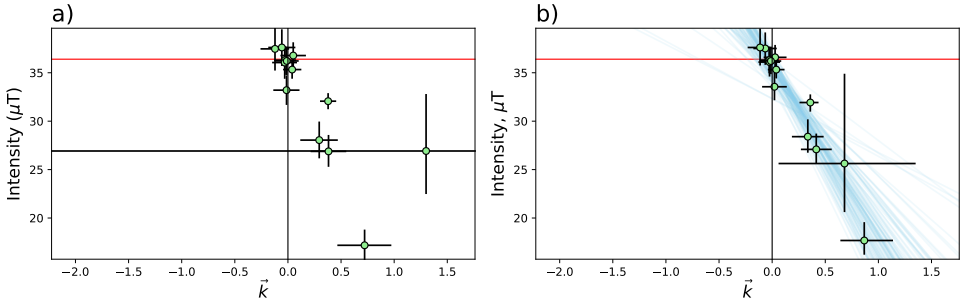

Figure S13. The same methodology described in the caption for Figure S3 applied to site hw126

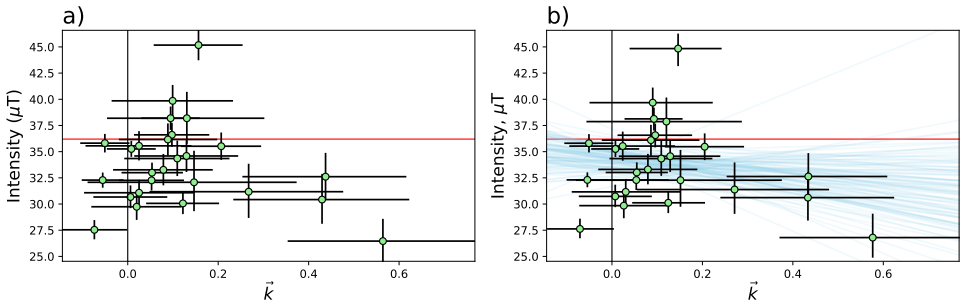

Figure S14. The same methodology described in the caption for Figure S3 applied to site hw128

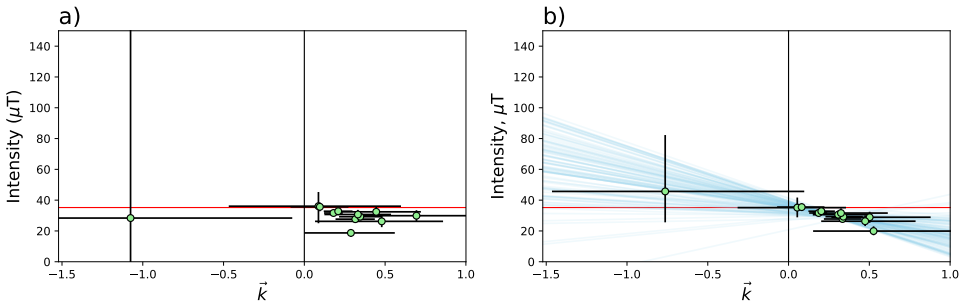

Figure S15. The same methodology described in the caption for Figure S3 applied to site hw201

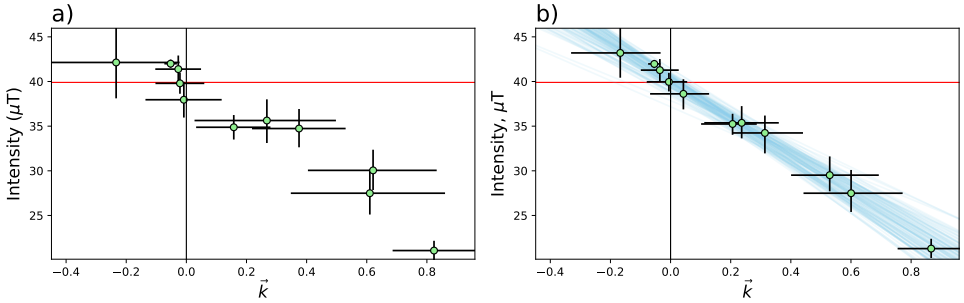

Figure S16. The same methodology described in the caption for Figure S3 applied to site hw226

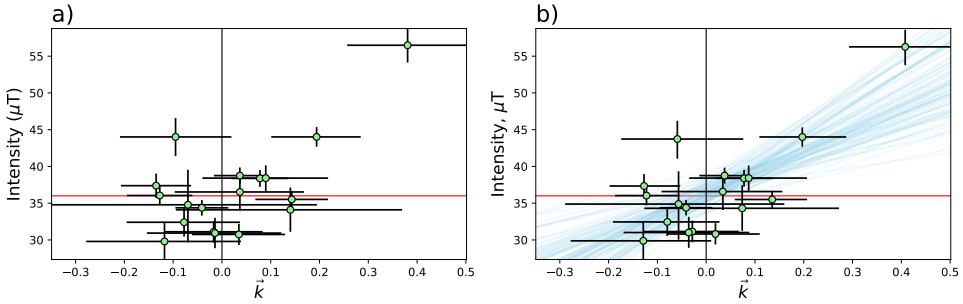

Figure S17. The same methodology described in the caption for Figure S3 applied to site hw241

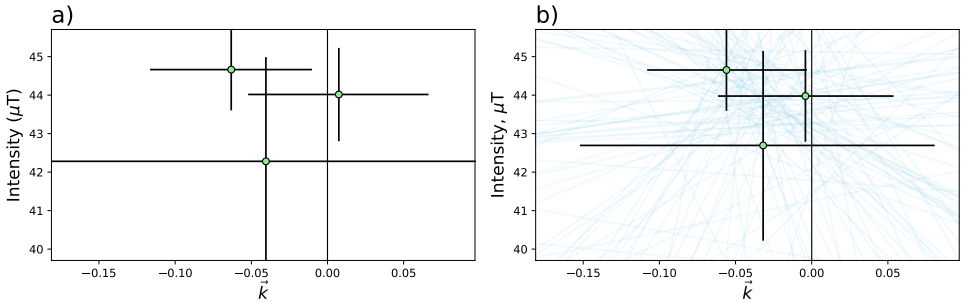

Figure S18. The same methodology described in the caption for Figure S3 applied to site kf

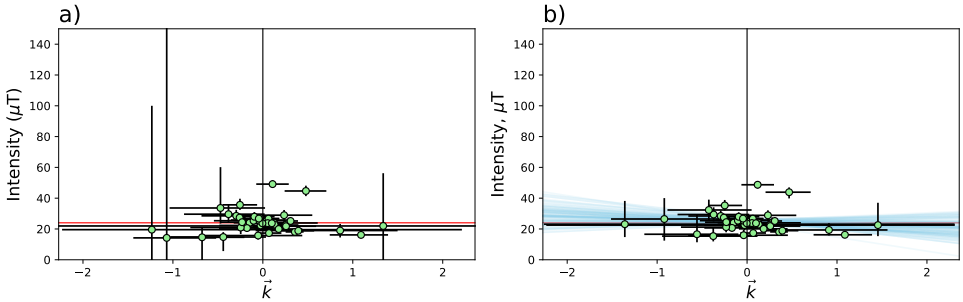

Figure S19. The same methodology described in the caption for Figure S3 applied to site LV

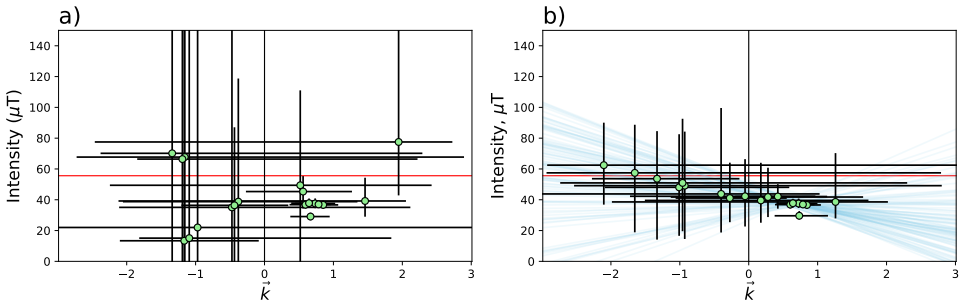

Figure S20. The same methodology described in the caption for Figure S3 applied to site MSH

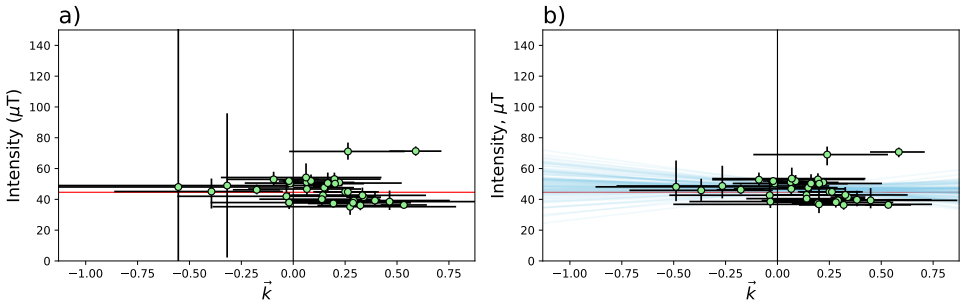

Figure S21. The same methodology described in the caption for Figure S3 applied to site P

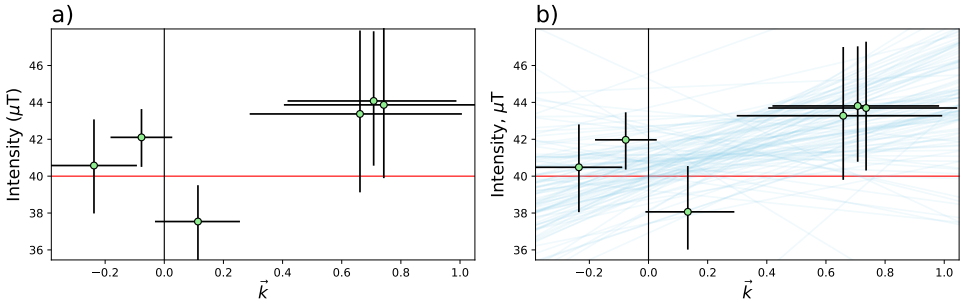

Figure S22. The same methodology described in the caption for Figure S3 applied to site remag-rs61

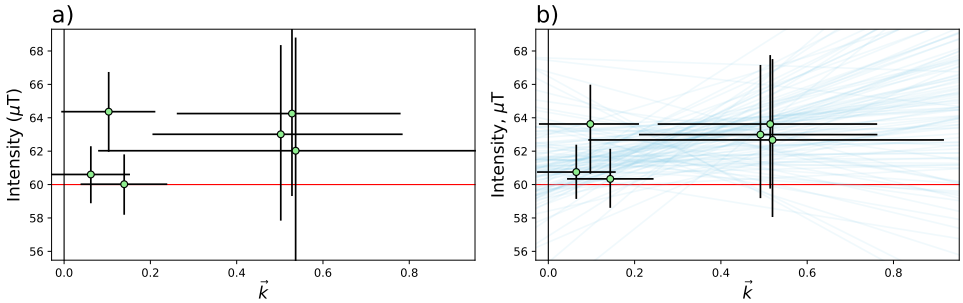

Figure S23. The same methodology described in the caption for Figure S3 applied to site remag-rs62

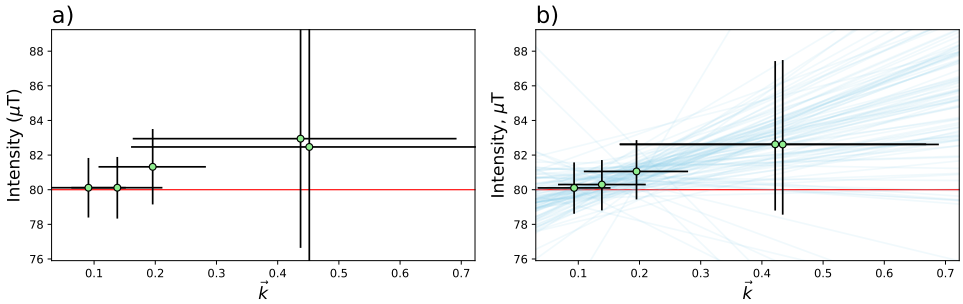

Figure S24. The same methodology described in the caption for Figure S3 applied to site remag-rs63

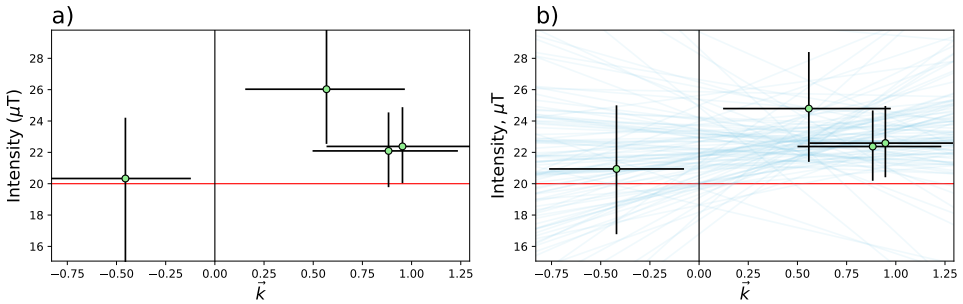

Figure S25. The same methodology described in the caption for Figure S3 applied to site remag-rs78

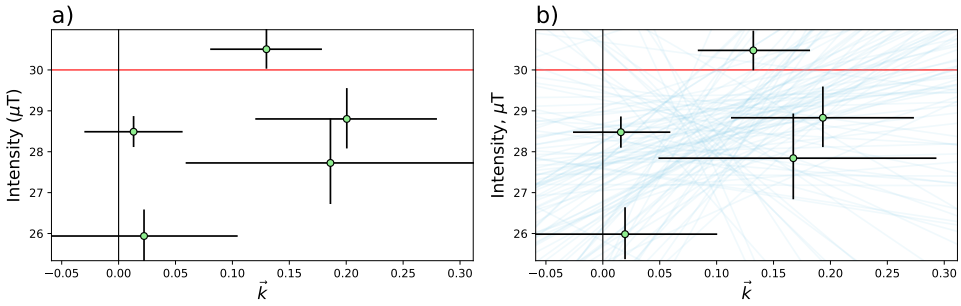

Figure S26. The same methodology described in the caption for Figure S3 applied to site rs25

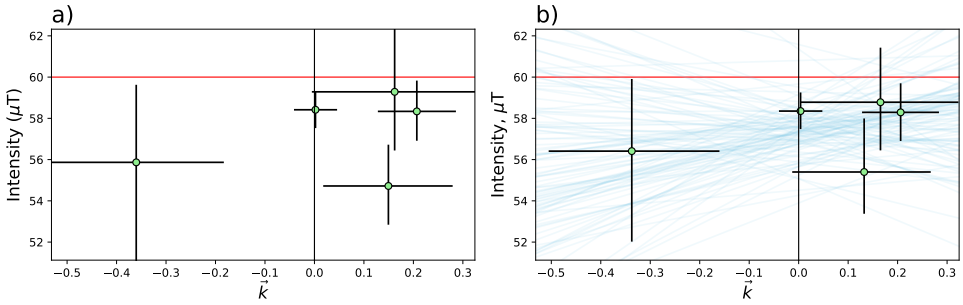

Figure S27. The same methodology described in the caption for Figure S3 applied to site rs26

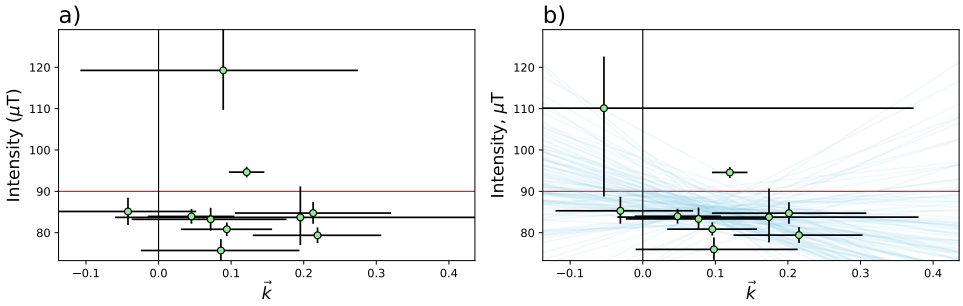

Figure S28. The same methodology described in the caption for Figure S3 applied to site rs27

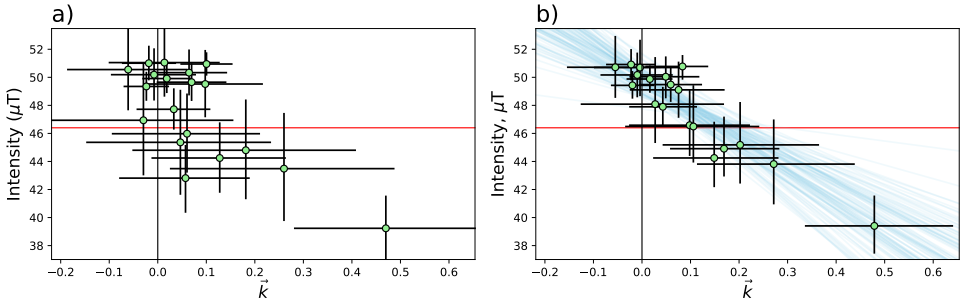

Figure S29. The same methodology described in the caption for Figure S3 applied to site SW

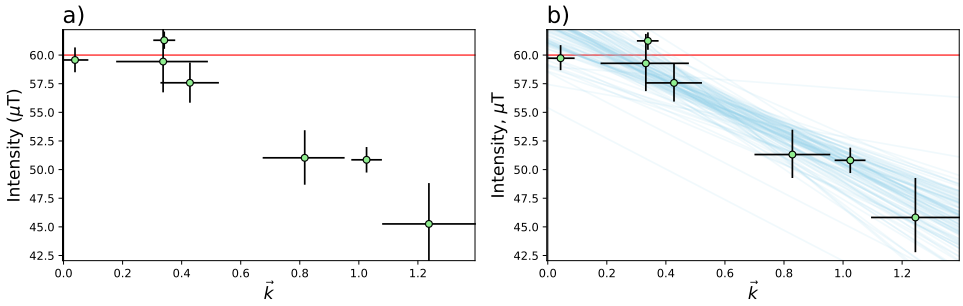

Figure S30. The same methodology described in the caption for Figure S3 applied to site Synthetic60

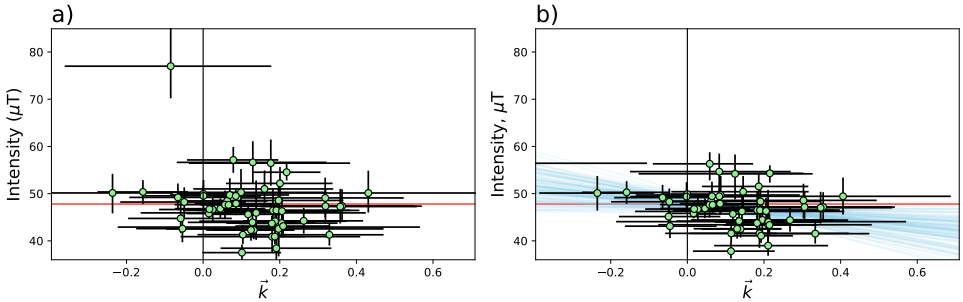

Figure S31. The same methodology described in the caption for Figure S3 applied to site TS

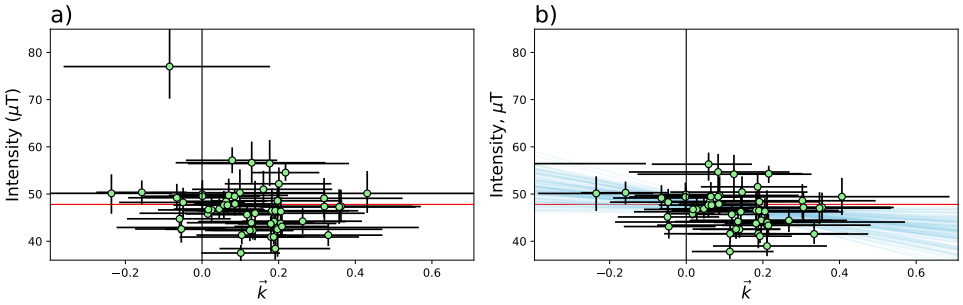

Figure S32. The same methodology described in the caption for Figure S3 applied to site VM